Appl Microbiol Biotechnol (2014) 98:351–360
DOI 10.1007/s00253-013-5372-1

GENOMICS, TRANSCRIPTOMICS, PROTEOMICS

Allantoin catabolism influences the production of antibiotics in *Streptomyces coelicolor*

Laura Navone · Paula Casati · Cuauhtémoc Licona-Cassani · Esteban Marcellin · Lars K. Nielsen · Eduardo Rodriguez · Hugo Gramajo

Received: 19 September 2013 / Revised: 28 October 2013 / Accepted: 30 October 2013 / Published online: 29 November 2013

Abstract Purines are a primary source of carbon and nitrogen in soil; however, their metabolism is poorly understood in *Streptomyces*. Using a combination of proteomics, metabolomics, and metabolic engineering, we characterized the allantoin pathway in *Streptomyces coelicolor*. When cells grew in glucose minimal medium with allantoin as the sole nitrogen source, quantitative proteomics identified 38 enzymes upregulated and 28 downregulated. This allowed identifying six new functional enzymes involved in allantoin metabolism in *S. coelicolor*. From those, using a combination of biochemical and genetic engineering tools, it was found that allantoinase (EC 3.5.2.5) and allantoicase (EC 3.5.3.4) are essential for allantoin metabolism in *S. coelicolor*. Metabolomics showed that under these growth conditions, there is a significant intracellular accumulation of urea and amino acids, which eventually results in urea and ammonium release into the culture medium. Antibiotic production of a urease mutant strain showed that the catabolism of allantoin, and the subsequent release of ammonium, inhibits antibiotic production. These observations link the antibiotic production impairment with an imbalance in nitrogen metabolism and provide the first evidence of an interaction between purine metabolism and antibiotic biosynthesis.

Keywords *Streptomyces* · Allantoin · Ammonium · Antibiotic regulation

Electronic supplementary material The online version of this article (doi:10.1007/s00253-013-5372-1) contains supplementary material, which is available to authorized users.

L. Navone · E. Rodriguez (✉) · H. Gramajo
Instituto de Biología Molecular y Celular de Rosario (IBR), Consejo Nacional de Investigaciones Científicas y Técnicas, Facultad de Ciencias Bioquímicas y Farmacéuticas, Universidad Nacional de Rosario, Suipacha 531, S2002LRK Rosario, Argentina
e-mail: erodriguez@ibr-conicet.gov.ar

P. Casati
Centro de Estudios Fotosintéticos y Bioquímicos (CEFOBI-Consejo Nacional de Investigaciones Científicas y Técnicas), Facultad de Ciencias Bioquímicas y Farmacéuticas, Universidad Nacional de Rosario, Suipacha 531, S2002LRK Rosario, Argentina

C. Licona-Cassani · E. Marcellin · L. K. Nielsen
Australian Institute for Bioengineering and Nanotechnology, The University of Queensland, Brisbane 4072, Australia

Introduction

Streptomyces species synthesize about half of all known antibiotics of microbial origin as well as metabolites with other important therapeutic and biotechnological applications (e.g., bleomycin, tetracycline, clavulanic acid, amphotericin B, avermectin, among others) (Omura and Oiwa 1984). The importance of natural products in human health has stimulated many investigations to understand the biosynthesis and regulation of natural products in *Streptomyces* species. However, much less effort has been put in understanding the influence of primary over secondary metabolism, particularly on the mechanism of catabolism of abundant carbon and nitrogen sources found in their natural environment. Moreover, very few investigations have studied in detail the metabolism of different carbon and nitrogen sources and their contributions to the production of biotechnological relevant compounds (Hodgson 2000).

Among the carbon and nitrogen sources found in the natural environment of streptomycetes, purines and their derivatives are highly abundant. Purines arise from decaying tissues and dead organisms or are secreted by living organisms such as animals and plants. The release of purines or allantoin into

the soil changes the nutrient composition of the soil and in consequence the microbial community. Increased levels of purines result in increased microbial diversity as well as living microbial biomass (Wang et al. 2010; Wang et al. 2007). Therefore, purine metabolism must play an important role in soil microoraganisms, not only in recycling carbon and nitrogen compounds but also in regulating microbial metabolism.

While the ability to degrade purines has been described in all kingdoms, the catabolic pathway diverges greatly among different organisms (Nygaard 1983; Vogels and Van der Drift 1976). Some organisms are capable of degrading purines to carbon dioxide and ammonium, while others, with an incomplete purine degradation pathway, excrete intermediates such as uric acid or allantoin (Vogels and Van der Drift 1976). *Streptomyces* spp. have been reported to contain the purine salvage pathway, which allows them to maintain the homeostasis of purine content, and also a catabolic pathway that allows them to use hypoxanthine as sole nitrogen source (Hodgson 2000). However, to date, only three enzymes namely, hypoxanthine phosphoribosyltransferase, xanthine oxidase, and uricase, have been characterized in *Streptomyces coelicolor* and *Streptomyces cyanogenus* (Ohe and Watanabe 1980; Ohe and Watanabe 1981; Watanabe 1971). Hypoxanthine phosphoribosyltransferase converts inosine-5′-phosphate into hypoxanthine (Ohe and Watanabe 1980). Hypoxanthine oxidation to uric acid is catalyzed by xanthine oxidase in two steps. The first step is the oxidation of hypoxanthine to xanthine followed by a second oxidation of xanthine to uric acid (Ohe and Watanabe 1979; Ohe and Watanabe 1981). Subsequently, uric acid is oxidized to allantoin via three enzymatic steps, in which only uricase has been characterized (Watanabe 1971). Here, we used proteomics, genetic engineering, and biochemical enzyme characterizations to elucidate the pathway for allantoin catabolism in *S. coelicolor*. Finally, metabolomics showed that allantoin metabolism produced an imbalance of nitrogen compounds with marked consequences on antibiotic production.

Materials and methods

Strains and growth conditions

DNA cloning and manipulation were performed in *Escherichia coli* DH5α while *E. coli* BL21 (DE3) was used for protein expression. *E. coli* strains were grown either on solid or in liquid Luria–Bertani medium at 37 °C and supplemented with the following antibiotics: 100 mg l^{-1} ampicillin (Ap), 50 mg l^{-1} kanamycin (Km), 20 mg chloramphenicol (Cm), or 100 mg l^{-1} apramycin (Am) when needed. *S. coelicolor* strain M145 ($SCP1^{-}$ $SCP2^{-}$) (Kieser et al. 2000) was grown at 30 °C on soya-mannitol agar or liquid minimal medium containing 20 mM allantoin (MM-A), 1 % glucose and 20 mM allantoin (MM-GA), and/or 0.2 % casamino acids (MM-GC) as nitrogen source, as indicated in the text (Kieser et al. 2000). For *Streptomyces* selection, the antibiotics Am, hygromycin (Hyg), and Km were added to solid or liquid medium at final concentrations of 50 mg l^{-1}.

Cloning of allB and alc genes

allB (sco6247) and *alc* (sco6248) were amplified by PCR from genomic *S. coelicolor* M145 DNA using the following oligonucleotides: for *allB*, 5′-**CATATG**TCCGAAGCTG AACTG-3′ (upper) and 5′-**GAATTCACTAGT**TCAG GCCCGGTCGAG-3′ (lower) and for *alc*, 5′-**CATA TG**GACGGCCCAGCAGAACAC-3′ (upper) and 5′-**GAAT TCACTAGT**CAGCCGCCCAGTTCCTGG-3′ (lower). The upper primers used were designed to have an *Nde*I site (boldface) overlapping the translational initiation codon, changing GTG start codons to ATG for both genes. The lower primers contained *Eco*RI and *Spe*I sites (boldface) downstream of the stop codon. The resulting PCR products were verified by DNA sequencing and cloned as *Nde*I-*Eco*RI fragments into the expression vector pET28a, which contains six His codons upstream of the *Nde*I site, to obtain pET28a::6247 (pLN03) and pET28a::6248 (pLN05), respectively. For complementation in *S. coelicolor*, each *Nde*I-*Spe*I fragment from pLN03 and pLN05 was cloned into the integrative vector pTR802 containing the *allB* promoter to make pLN06 (c_*allB*), pLN07 (c_*alc*), and pLN09 (c_*allB*-*alc*), respectively.

Expression and purification of AllB and Alc

E. coli BL21 (DE3) host strains (Stratagene) carrying plasmids pLN03 or pLN05 were grown at 37 °C in Terrific Broth medium supplemented with 1 mM $CoCl_2$ (Mulrooney and Hausinger 2003) or Luria–Bertani medium, respectively, induced with 0.5 mM isopropyl-D-thiogalactopyranoside (IPTG), and incubated for 20 h at 30 °C. Cells were harvested by centrifugation at 4,000×*g* for 20 min at 4 °C, washed twice, and resuspended in buffer containing 50 mM Tris–HCl (pH 7.0), 150 mM NaCl, 10 % glycerol, and 10 mM $MgCl_2$ (buffer A). Cell disruption was carried out in a French pressure cell at 1,000 MPa in the presence of 0.1 % (*v*/*v*) protease inhibitor cocktail (Sigma-Aldrich). The protein extract was cleared by centrifugation at 15,000×*g* for 30 min at 4 °C, and the supernatant applied to a Ni_2-nitrilotriacetic acid–agarose affinity column (Qiagen) equilibrated with the same buffer supplemented with 20 mM imidazole. The column was washed, and the His-tagged proteins eluted using buffer A containing 60–250 mM imidazole. Fractions were collected and analyzed by sodium dodecyl sulfate–polyacrylamide gel electrophoresis. Fractions containing purified proteins were dialyzed overnight using buffer A at 4 °C. Pure proteins were stored at −80 °C.

Allantoinase and allantoicase enzyme assays

For determination of allantoinase activity, the reaction mixture contained 50 mM allantoin, 50 mM triethanolamine–HCl (pH 8.2), and the enzyme in a final volume of 0.36 ml. After incubation at 30 °C, 0.5 ml of 0.5 N HCl was added and the reaction mixture was placed in a boiling water bath for 2 min to hydrolyze the allantoic acid formed to glyoxylate. It was then cooled in an ice bath and buffered by the addition of 0.5 ml of 0.5 M of phosphate potassium buffer pH 7.5. Glyoxylate was determined by using lactate dehydrogenase and NADH (Takada and Noguchi 1983). Allantoicase activity was determined using allantoic acid as substrate by measuring the formation of urea as a function of time, using a commercial kit (Urea Color 2R, Wiener Lab). Briefly, the reaction was assayed at 30 °C in 0.5 ml reaction volume containing 50 mM triethanolamine–HCl buffer (pH 8.2) and 50 mM allantoic acid. At each time point, a 50-μl aliquot was taken and boiled for 5 min to stop the enzyme reaction. For urea determination, 1 μl of this aliquot was mix with 100 μl of a reagent containing 200 mM phosphate buffer, 750 mM salicylic acid, 20 mM sodium nitroprussate, and 10 mM EDTA along with urease solution of 75 U ml^{-1}. After 5 min of incubation at 37 °C, the reaction was stopped with 100 μl of 10 mM sodium hypochlorite in 0.1 M sodium hydroxide. After incubation at 37 °C for 5 min, the ammonium formed was determined by spectrophotometry at 570 nm. For determination of allantoinase kinetic parameters, allantoin concentration varied from 2.5 to 90 mM. One unit of enzyme activity is defined as the amount of enzyme resulting in the production of 1 μmol of urea per minute.

Isolation of $AllB^-$, Alc^-, $AceB1^-$, Gcl^-, and $UreB^-$ mutant strains of *S. coelicolor*

To disrupt *allB*, *alc*, *aceB1* (sco6243), *gcl* (sco6201), and *ureB* (sco1235), four cosmids from the transposon insertion cosmid library of *S. coelicolor* were used (Herron et al. 2004). Cosmids AH10.1.F09, 2H4.2.G01, 2H4.2.A10, SC2G5.2.F07, and 2STG1.1.A10 carrying individual Tn5062 insertions in each gene were introduced into *S. coelicolor* M145 by conjugation using *E. coli* ET12567/pUB307 as a donor (Rodriguez et al. 2003). For each mutant, two independent Am^R Km^S exconjugants were isolated and checked by PCR using specific primers for each gene and for the transposon, verifying that allelic replacement had occurred.

Antibiotic determinations

Antibiotic determinations were performed as described previously (Bystrykh et al. 1996; Tsao et al. 1985).

RNA extraction and real-time qRT-PCR assay

RNA was extracted from M145 grown for 24 or 46 h in MM-GC and MM-GA liquid medium using the SV total RNA isolation system (Promega). Second-strand cDNA was synthesized using SuperScript III Reverse Transcriptase (Invitrogen) with random primers and used in quantitative PCR (qPCR) with SYBR green as the indicator dye. Primer pairs RThrdBR (5′-GTTGATGACCTCGACCATGT-3′) and RThrdBL (5′-CAAGGGCTACAAGTTCTCCA-3′), RTactIIORF4R (5′-TACACGAGCACCTTCTCACC-3′) and RTactIIORF4L (5′-TGGAATCGTATCGGAATCTC-3′), and RTaceB1R (5′-CGGAAGTTCTTGACGATG-3′) and RTaceB1L (5′-GGAACGAGGTCTTCGTCGTCTT-3′) were used to analyze transcript levels of *hrdB*, *actII*-ORF4, and *aceB1*, respectively. The expression of each gene was quantified after normalization to *hrdB* mRNA levels. qPCR was carried out in an Eppendorf Realplex^2 PCR machine using the following cycling conditions: 95 °C for 2 min followed by 40 cycles at 94 °C for 15 s, 58 °C for 15 s, and 68 °C for 20 s. qPCR data are presented as a fold difference of expression in M145 cells grown in MM-GC relative to that in M145 cells grown in MM-GA using the Pfafll method (Pfaffl 2001), with *hrdB* used as a normalizing gene.

Urea and ammonium determinations

Urea and ammonium were measured using a commercial kit (Urea Color 2R, Wiener Lab). To measure ammonium concentration, urease solution was not added to the reaction mixture.

Isobaric tags for relative and absolute quantification (iTRAQ) labeling

Cells from exponential and stationary phase grown in 50 ml MM-GC or MM-GA medium were harvested in duplicates by filtration with 0.45-μm nitrocellulose membrane, washed with PBS solution (pH 7.5) (8 g NaCl, 0.2 g KCl, 1.44 g Na_2PO_4, 0.24 g KH_2PO_4 per liter), and resuspended in lysis buffer (50 mM Tris–HCl (pH 7.5), Thermo protease inhibitor). To obtain homogeneous cell disruption, cells were disrupted by sonication and cellular debris was removed by centrifugation (10,000×*g* 10 min at 4 °C). To further remove impurities, DNase I (Fermentas) and RNase A (Fermentas) were added to the lysate. The crude protein extract was extensively dialyzed against Milli-Q water and concentrated by lyophilization. Lyophilized proteins were trypsin digested and labeled with iTRAQ reagents as described by the manufacturer's protocol. Briefly, 50 μg of protein from each condition and two biological replicates were reduced with 50 mM tris (2-carboxyethyl) phosphine (TCEP) at 60 °C for 1 h and cysteine residues alkylated with 200 mM methyl methane-thiosulphonate

(MMTS) at room temperature for 15 min. Enzymatic digestion was performed with trypsin (Promega, Gold trypsin; 1:20, *w*/*w*) at 37 °C for 16 h. Labeling was performed for 2 h with one isobaric amine-reactive tag per sample and labeled samples were pooled, evaporated to dryness in a vacuum centrifuge, resuspended in SCX buffer (10 mM K_2HPO_4 25 % CAN, pH=2.7), and cleaned to remove the reducing reagent, SDS, calcium chloride, and excess iTRAQ using a cation exchange cartridge system from AB Sciex.

Liquid chromatography coupled to mass spectrometry (LC-MS) analysis

Samples were then analyzed using a nano-LC hybrid TripleTOF 5600 (AB-Sciex) equipped with a Shimadzu Prominence nano-LC system. The LC was equipped with a C_{18} column (Vydac MS C18 300 Å 150×0.3 mm, GRACE Davison, Discovery Sciences, USA) operated at 30 °C with a gradient running from 0 to 80 % acetonitrile (in 0.1 % formic acid) for 220 min at a flow rate of 3 μl/min. Peptides were sprayed with a Nano-ESI III source. Gas and voltage settings were adjusted as required. Proteins were identified by information-dependent acquisition of the fragmentation spectra of 1–4 charged peptides with a precursor selection window of 100 to 1,800 *m*/*z* using enhanced pulsed extraction of fragments for 0.5 s followed by data-dependent acquisition of 20 peptides with intensity above 100 counts across *m*/*z* 40–1,800 (0.05 s per spectrum) with rolling collision energy. Peptides were identified using the paragon algorithm using FASTA formatted protein sequences for the finished *S. coelicolor* genome obtained from NCBI (Protein Pilot software 4.0, Applied Biosystems) (Shilov et al. 2007). Search parameters included trypsin as enzyme, MMTS as cys-modification, and "thorough" search setting. Only proteins with a ProteinPilot confidence score of 95 % or better (estimated global FDR 5 % or lower) were accepted. Ratios for iTRAQ and *p* values were performed using the Paragon method described elsewhere (Shilov et al. 2007).

Results

Proteomics analysis of *S. coelicolor* grown in allantoin

Previous studies have shown that *Streptomyces* spp. can utilize purines and hypoxanthine as nitrogen sources (Hodgson 2000). However, the pathway for purine degradation beyond allantoin remains elusive. As a first approach, we used a combination of proteomics and genetic engineering to characterize key enzymes involved in allantoin metabolism in *S. coelicolor* M145. Thus, we grew this microorganism in minimal medium containing allantoin as the sole carbon and nitrogen source (MM-A) or in minimal medium containing glucose and allantoin as carbon and nitrogen sources, respectively (MM-GA). As a control, cells were grown in minimal medium containing glucose and casamino acids (MM-GC) (Fig. 1a). Growth analysis showed that *S. coelicolor* M145 can metabolize allantoin as nitrogen and carbon source; however, the slow growth in MM-A showed that the medium supplemented with glucose and allantoin (MM-GA) was more suitable for further experiments.

In order to identify proteins involved in allantoin metabolism, we compared the proteome of *S. coelicolor* M145 grown in MM-GA to the proteome of cells grown in MM-GC. Culture samples were collected from each medium at two different time points and proteins were extracted, labeled, and analyzed by LC-MS using iTRAQ. More than 450 proteins (with at least two peptides with 99 % confidence) were identified. Approximately 70 of these proteins showed statistically significant changes in their expression levels during the exponential and stationary phases of growth (Table S1,

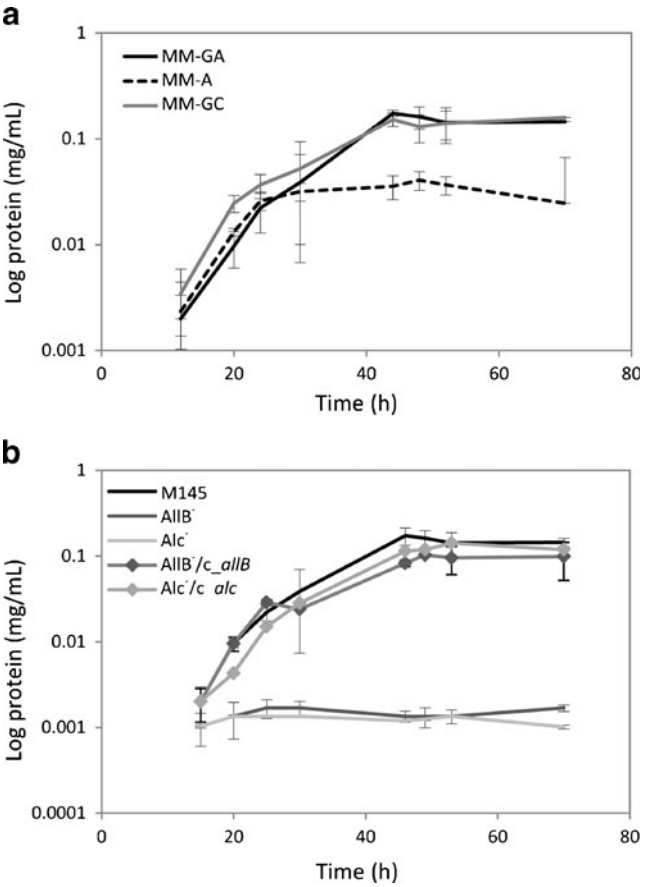

Fig. 1 **a** Analysis of *S. coelicolor* M145 minimal medium supplemented with allantoin (MM-GA) or casamino acids (MM-GC) as sole nitrogen source and in minimal medium supplemented with allantoin as sole carbon and nitrogen source (MM-A). **b** Analysis of *S. coelicolor* M145 and of the $AllB^-$ and Alc^- mutant strains growing in glucose minimal medium supplemented with allantoin (MM-GA) as sole nitrogen source. $AllB^-$/c_*allB* and Alc^-/c_*alc* correspond to the complemented mutant strains: $AllB^-$ with *allB* gene and Alc^- with *alc* gene, respectively. Results represent the average of three independent experiments ± SD

supplementary materials). Half of the proteins with more than a fourfold increase in expression were found when *S. coelicolor* grew on allantoin as the sole nitrogen source. These proteins were selected as candidate enzyme to elucidate the catabolic pathway of allantoin (Table 1, shown in green in Fig. 2). For example, the levels of allantoicase (Alc), tartronate semialdehyde reductase (GlxR), glyoxylate carboligase (Gcl), hydroxypyruvate isomerase (Hyi), and malate synthase (AceB1) (Bentley et al. 2002; Loke and Sim 2000) were significantly higher at the exponential phase when cells were grown in MM-GA compared with the levels found in MM-GC (6.2, 10.4, 9.3, 8.8, and 3.9-fold, respectively). In addition, a putative ureidoglycolate lyase (Ugl) was also detected with a 2.2-fold increased level in MM-GA. Similarly, the protein Sco6204 was upregulated when cells grew in allantoin (6.3-fold); this ORF showed strong similarity to a catalase enzyme previously characterized (Bentley et al. 2002). Furthermore, most of these proteins also showed increased levels of expression in M145 grown in MM-GA during stationary growth phase (Table S1, supplementary materials).

Proteomics also showed changes in protein levels when cells grew in allantoin as the sole nitrogen source (Fig. 2, Table S1, supplementary materials): namely, glutamate uptake system ATP-binding protein (GluA), glutamate periplasmic-binding protein (GluB), and glutamine synthase II (GSII) were downregulated during the exponential growth phase in MM-GA (showed in red in Fig. 2).

Proteins involved in carbon metabolism also showed different levels of expression subject to the source of nitrogen used. A clear example was the malate dehydrogenase (Mdh) enzyme, which was the only tricarboxylic acid cycle (TCA) enzyme that showed an increase in its expression during growth in medium supplemented with allantoin. The increased expression of this enzyme during stationary phase is likely to be the result of high quantities of malate generated by allantoin catabolism (Table S1, supplementary materials). Additional TCA enzymes (2-oxoglutarate dehydrogenase (sco5281), succinyl-CoA synthetase (SucD and SucC), citrate synthase (CitA), and isocitrate dehydrogenase (Idh) showed a decrease in expression during growth in MM-GA relative to MM-GC at 24 h of growth (Table S1, supplementary materials).

Characterization of the allantoin catabolic pathway

Based on proteomics and bibliomic data, we proposed a new pathway for allantoin metabolism in *S. coelicolor* (Fig. 2). The pathway involves five proteins: Alc, GlxR, Gcl, Hyi, AceB1, and Ugl (Fig. 2). Analysis of the *S. coelicolor* genome also revealed an operon coding for a putative allantoinase (AllB) adjacent to *alc* (Bentley et al. 2002). Therefore, we included this enzyme in our gene candidates for genetic engineering to elucidate the pathway (Fig. 2). Mutant strains were isolated for *allB*, *alc*, *aceB1*, and *gcl* genes using molecular biology techniques described earlier (Herron et al. 2004).

To compare the effect on growth, as well as on antibiotic production, the parental strain and each of the mutant strains generated were grown in minimal medium supplemented with different carbon and nitrogen sources in shake flasks. The AceB1$^-$ and Gcl$^-$ mutants showed no difference in growth compared to the parental strain in all media tested (data not shown). This result suggested that these two enzymes represent alternative branches of glyoxylate metabolism as shown in Fig. 2. However, neither AllB$^-$ nor Alc$^-$ mutant strains were able to grow in glucose minimal medium with allantoin as the nitrogen source (Fig. 1b). To verify these results, each mutant strain was complemented with the integrative plasmid pRT802 containing a wild-type copy of the corresponding gene (Herron et al. 2004). As shown in Fig. 1b, the expression of a wild-type copy of the *allB* or *alc* gene in the corresponding mutant strain restored growth on allantoin. This result

Table 1 Proteins showing increased levels in MM-GA and containing significant homology to known allantoin metabolic enzymes

Protein	Closest protein match[a]	Sim[b] (%)	Function	r[c]	Reference
GlxR, SCO6205	GlxR (*E. coli*)	43	Tartronate semialdehyde reductase	10.44	(Njau et al. 2000)
Hyi, SCO6206	Hyi (*E. coli*)	34	Hydroxypyruvate isomerase	9.35	(Ashiuchi and Misono 1999)
Gcl, SCO6201	Gcl (*E. coli*)	73	Glyoxylate Carboligase	8.88	(Gupta and Vennesland 1964)
SCO6204	KatE (*E. coli*)	48	Catalase	6.32	(Loewen and Switala 1986)
Alc, SCO6248	PuuF (*Pseudomonas aeruginosa*)	39	Allantoicase	6.23	(Trijbels and Vogels 1966)
AceB1, SCO6243	AceB (*E. coli*)	49	Malate synthase	3.99[d]	(Molina et al. 1994)
Ugl, SCO2850	Ugl (*Burkholderia cepacia*)	54	Ureidoglycolate lyase	2.19	(McIninch et al. 2003)

Sim similarity

[a] Characterized proteins involved in allantoin metabolism

[b] Determined by BLASTP using default parameters

[c] Ratio of protein level detected in MM-GA/MM-GC. Student's t test, $P<0.1$

[d] Validated by RT-PCR (Table S2)

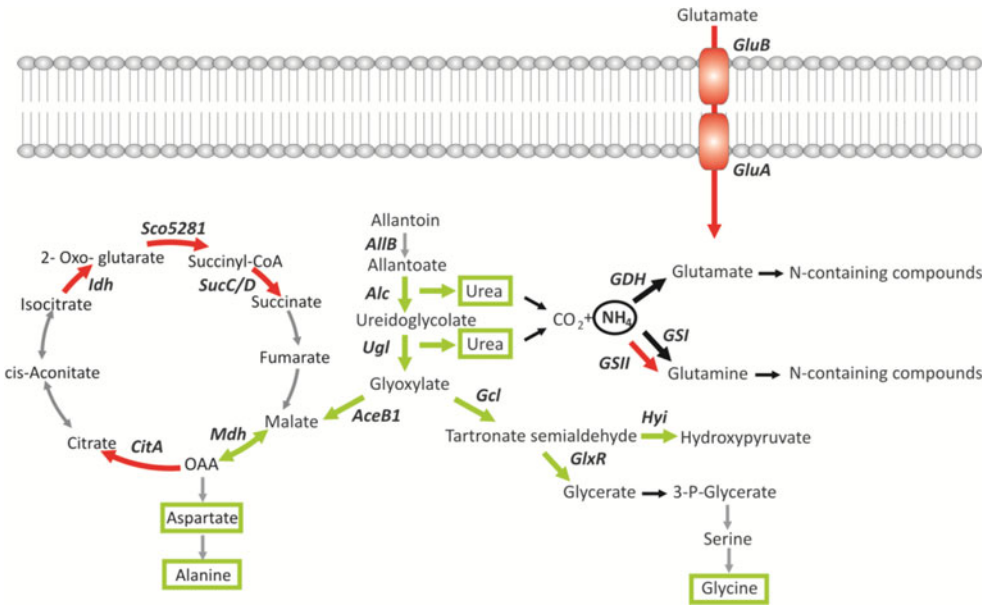

Fig. 2 Allantoin catabolic pathway proposed for *S. coelicolor*. The effect on proteins and metabolite levels related to the allantoin pathway found in *S. coelicolor* M145 are indicated in *color*. *Green arrows* represent proteins with increased levels in MM-GA relative to MM-GC, *red arrows* represent proteins with decreased levels in MM-GA relative to MM-GC, *black arrows* represent proteins with no alteration in expression levels and *gray arrows* represent proteins not detected in the assay. *Boxes* correspond to those metabolites that showed increased intracellular quantities in MM-GA medium relative to MM-GC medium

indicates that both AllB and Alc proteins form the unique metabolic pathway involved in allantoin catabolism.

Biochemical characterization of AllB and Alc proteins

To confirm the allantoinase activity of AllB and the allantoicase activity of Alc, both proteins were expressed as His-tag recombinant proteins in *E. coli* BL21 strain and purified using affinity chromatography. Biochemical assays confirmed that AllB catalyzes the conversion of allantoin to allantoate with a V_{max} of 619±25 U mg^{-1} and a K_m for allantoin of 41±4 mM. On the other hand, we confirmed that Alc catalyzes the conversion of allantoate to ureidoglycolate and urea with a V_{max} of 218±20 U mg^{-1}. The kinetic parameters estimated for each enzyme are comparable to the values reported for other bacterial orthologs (Mulrooney and Hausinger 2003; Piedras et al. 2000; Schultz et al. 2001). It is important to note that AllB was expressed in a medium supplemented with $CoCl_2$ for the purification of the enzyme in its native form. The presence of the divalent cation in the medium strongly increased allantoinase activity, as previously demonstrated in *E. coli* (Mulrooney and Hausinger 2003).

Effect of allantoin metabolism in antibiotic production

Surprisingly, when *S. coelicolor* grew in MM-GA a marked decrease in antibiotic production was observed. This effect was also observed in cultures grown in glucose minimal medium supplemented with casamino acids and allantoin as nitrogen sources (MM-GCA). Both actinorhodin and undecylprodigiosin were produced at lower levels in cells grown in MM-GCA (Fig. 3). To find out whether these results were a consequence of the addition of allantoin or were linked to the metabolism of this compound, we measured the level of antibiotics production for the AllB$^-$ and Alc$^-$ mutants in MM-GCA. In contrast to the results observed in the wild-type

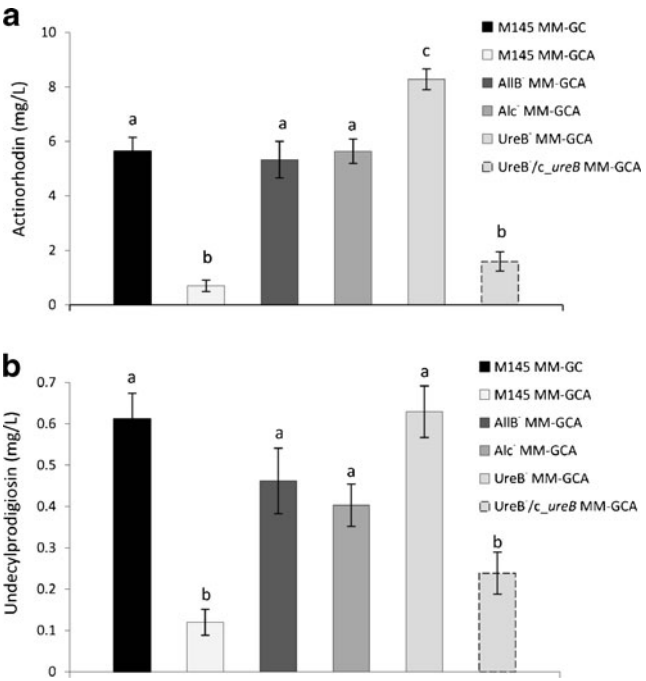

Fig. 3 **a** Quantitation of actinorhodin production by *S. coelicolor* M145, AllB$^-$, Alc$^-$, and UreB$^-$ mutant strains at 72 h of growth on glucose minimal medium supplemented with casamino acids (MM-GC) or with casamino acids and allantoin as indicated (MM-GCA). **b** Quantification of undecylprodigiosin production by *S. coelicolor* M145, AllB$^-$, Alc$^-$, and UreB$^-$ mutant strains at 60 h of growth in glucose minimal medium supplemented with casamino acids (MM-GC) or with casamino acids and allantoin as indicated (MM-GCA). Results represent the average of three independent experiments ± SD. *Different letters* denote statistical differences applying an ANOVA test using Sigma Stat 3.1 ($P<0.05$)

strain, the AllB$^-$ and Alc$^-$ mutant strains produced the same amount of actinorhodin and undecylprodigiosin as the wild-type strain grown without allantoin supplementation (MM-GC) (Fig. 3). These results confirm that the reduced levels of antibiotic production are due to allantoin metabolism and not to the presence of allantoin in the medium. This effect on antibiotic biosynthesis may be associated with the lack of precursor supply or to the regulation of expression of the antibiotic gene clusters. Expression level analysis of the gene encoding the transcriptional activator of the actinorhodin gene cluster (*actII*-ORF4) showed a 70-fold decrease in MM-GA relative to its expression in MM-GC, which confirms that actinorhodin production was due to a downregulation of *actII*-ORF4 expression by allantoin or any of its catabolic products (Table S2, supplementary materials). This result shows that the catabolism of allantoin causes metabolic changes that influence the expression of secondary metabolites such as actinorhodin.

Analysis of *S. coelicolor* grown in allantoin using metabolomics

The link between allantoin catabolism and antibiotic production was also analyzed using metabolomics, as described previously (Rodriguez et al. 2012). We analyzed the metabolic profiles of WT *S. coelicolor* grown in MM-GA or MM-GC at two time points: one during exponential and one at stationary phases of growth. Sixteen out of 40 intracellular metabolites showed statistically significant changes depending on the nitrogen source used (Table S3, supplementary materials). Interestingly, four nitrogen-containing metabolites (aspartate, alanine, glycine, and urea) showed increased concentration when *S. coelicolor* M145 was grown with allantoin as the nitrogen source (Fig. 4a). Among them, urea was remarkably the highest (83- and 453-fold increase, respectively, in MM-GA). In contrast, two other amino acids (glutamine and valine) showed slightly reduced levels under the same growth condition (Fig. 4b).

These results correlated well with the protein expression levels found during the stationary phase of growth (Table S1, supplementary materials). For example, 3-phosphoglycerate dehydrogenase (SerA) and a protein involved in serine and glycine biosynthesis showed a strong increase in its expression in MM-GA. This increase results in glycine accumulation during growth in MM-GA medium at 46 h (Fig. 4a). Furthermore, methylmalonic acid semialdehyde dehydrogenase (MsdA), and one enzyme of the valine degradation pathway, showed increased expression in MM-GA correlating with the decreased levels of valine (Fig. 4b).

Intracellular ammonium accumulation impairs antibiotic production

The high levels of intracellular urea detected when *S. coelicolor* grows in medium containing allantoin correlate

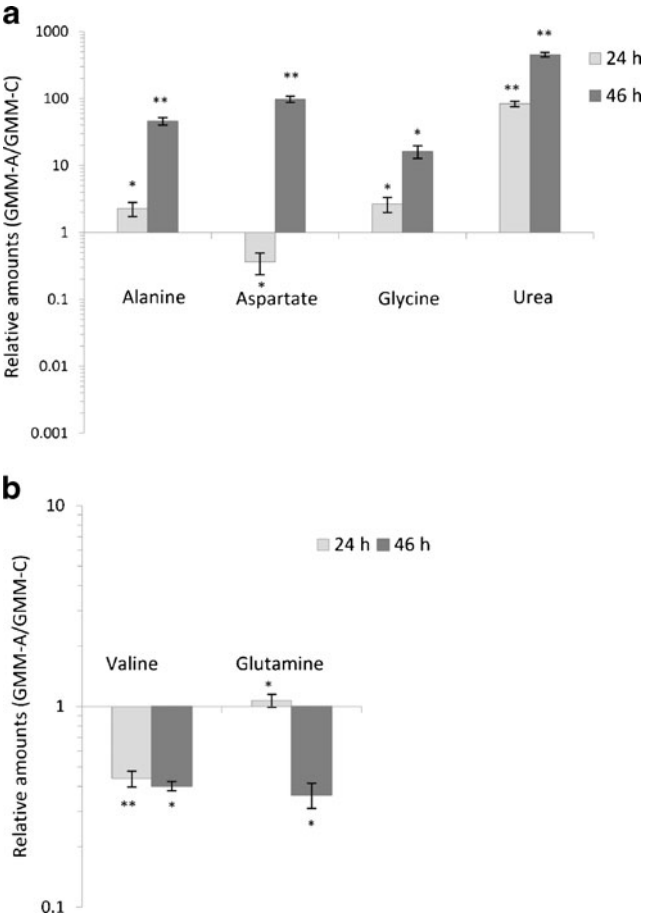

Fig. 4 Metabolic analysis of *S. coelicolor* M145 grown in glucose minimal medium supplemented with casamino acids (MM-GC) or allantoin (MM-GA) at exponential (24 h) and stationary phases of growth (46 h). Nitrogen-containing metabolites showed increased (**a**) or decreased (**b**) levels in MM-GA compared to MM-GC. Values represent mean differences between growth in MM-GA and MM-GC. Results represent the averages from three independent experiments ± SD. *Single asterisks* denote statistical differences applying student's *t* test ($P<0.1$) and double asterisks ($P<0.05$)

with the proposed metabolic pathway for allantoin catabolism proposed in this investigation (Fig. 2). In order to further validate this hypothesis, we quantified the urea and ammonium levels present in the culture supernatants. As shown in Fig. 5, both urea and ammonium concentrations increased in cultures grown in MM-GCA compared with MM-GC even during stationary phase of growth. These results suggest an absence of negative feedback regulation on the allantoin pathway, where excess nitrogen compounds, such as urea or ammonium, are excreted from the cells. Accumulation and release of high levels of intracellular ammonium due to allantoin catabolism may result in decreased levels of antibiotic production. To validate if the urease enzyme is in charge of breaking the urea molecules into ammonium and carbon dioxide in this pathway, we inactivated one gene encoding a putative subunit of the urease complex following the same strategy used for inactivating *allB* and *alc* (Herron et al.

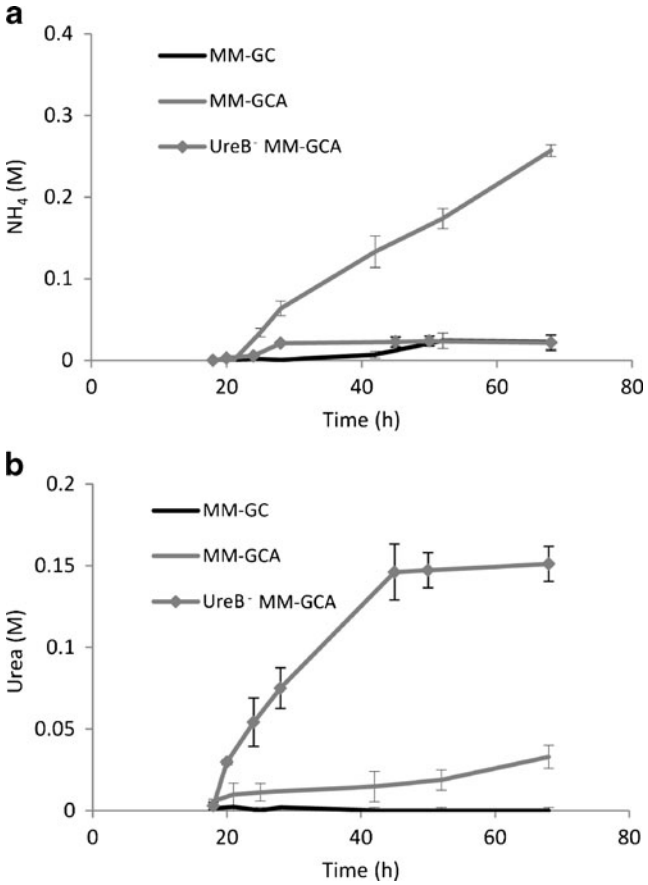

Fig. 5 Analysis of ammonium (**a**) and urea (**b**) levels in culture media after *S. coelicolor* M145 and UreB$^-$ mutant growth in glucose minimal medium supplemented with casamino acids (MM-GC) or casamino acids and allantoin (MM-GA). Results represent the averages from three independent experiments ± SD

2004). Using a cosmid carrying a mutant allele of Sco1235 (*ureB*) gene, we isolated a mutant strain and called it UreB$^-$. Urease activity assay in the protein extract of UreB$^-$ showed eightfold lower activity levels than in the M145 strain (Fig. S1). The UreB mutant showed no ammonium release in MM-GCA (Fig. 5a) and no decrease in antibiotic production under this condition (Fig. 3). This result strongly suggests that intracellular accumulation of ammonium could result in the downregulation of *actII*-ORF4 expression and therefore impair antibiotic production.

Discussion

In this work, we used a systematic proteomic approach to characterize the metabolic pathway for allantoin catabolism in *S. coelicolor*. This approach allowed us to identify six new functional enzymes of the allantoin pathway based on protein similitude against known allantoin metabolic enzymes from other bacteria. These proteins are allantoicase (Alc), malate synthase (AceB1), glyoxylate carboligase (Gcl), tartronate semialdehyde reductase (GlxR), hydroxypyruvate isomerase (Hyi), and ureidoglycolate lyase (Ugl). Although other allantoin pathways have been characterized in other bacterial systems, the specific set of enzymes employed by each particular microorganism differs considerably. For instance, allantoinase (Mulrooney and Hausinger 2003), malate synthase (Molina et al. 1994), glyoxylate carboligase (Gupta and Vennesland 1964), tartronate semialdehyde reductase (Njau et al. 2000), and hydroxypyruvate isomerase (Ashiuchi and Misono 1999) are present in *E. coli*, while allantoicase (Trijbels and Vogels 1966) and ureidoglycolate lyase (McInnch et al. 2003) are present in *Pseudomonas aeruginosa* and *Burkholderia cepacia*. Allantoinase activity is also present in *P. aeruginosa* and *B. cepacia*; however, PuuE allantoinase protein is a paralogous of AllB found in *E. coli* (Ramazzina et al. 2008).

Here, AllB and Alc were biochemically characterized, confirming that the two enzymes have allantoinase and allantoicase activities, respectively. AllB showed similar cation requirement to other previously characterized allantoinases (Mulrooney and Hausinger 2003). Genetic inactivation of these two enzymes demonstrated that these proteins constitute the sole pathway to metabolize purines in *S. coelicolor*.

When *S. coelicolor* M145 was grown using allantoin as nitrogen source, a notable decrease in antibiotic production was observed. This could be the result of an increase in pH linked to the ammonium released into the medium. However, a fivefold increase in buffer concentration did not restore antibiotic production (data not shown), suggesting that the intracellular accumulation of nitrogen (mainly ammonium) when *S. coelicolor* was grown in allantoin-containing media could be responsible for the impaired antibiotic production. The normal antibiotic production levels and the absence of ammonium in the culture medium of the UreB$^-$ mutant strain (grown in presence of allantoin) suggest that the excess of intracellular ammonium generated during degradation of allantoin causes a strong impairment of actinorhodin and undecylprodigiosin biosynthesis (Fig. 3). Several studies have found that nitrogen controls a number of pathways involved in secondary metabolism (Omura et al. 1983; Hobbs et al. 1990). In most cases, nitrogen excess causes a decrease in antibiotic production that may be due to repression of enzymes of the biosynthetic pathway (Brana et al. 1985; Shen et al. 1984). Alternatively, high nitrogen concentrations may affect enzymes that synthesize precursors for secondary metabolite production. While the specific molecular basis of this regulation is not well understood (Brana et al. 1986), it has been proposed that nitrogen limitation is necessary for either full expression of biosynthetic genes or full enzyme activity for actinorhodin production in *S. coelicolor* (Doull and Vining 1990). This tight link between nutrient availability and antibiotic production is not surprising. Several studies have shown that antibiotics, and in general, secondary metabolites, are

produced by the cells as a response to environmental cues. In this regard, we propose that excess ammonia signals nutrient richness and stimulate growth rather than production of secondary metabolites.

Given that excess of urea and ammonium are produced by allantoin degradation, we speculate that the allantoin pathway is not negatively regulated as found in other catabolic pathways. Our proteomic analysis supported this statement with the observation of significant changes in the expression levels of proteins for nitrogen uptake and assimilation (Fig. 2, Table S1, supplementary materials).

Indeed, others have also observed upregulation of the genes of the allantoin pathway during programmed cell death (PCD) (Manteca et al. 2006). PCD is triggered by nonspecific nucleases that degrade chromosomal DNA into free nucleotides. These nucleotides can then be used as carbon and nitrogen sources by the surviving population. In this respect, the activation of the purine catabolic enzymes in coordination with the allantoin pathway during PCD will degrade nucleotides completely into reduced carbon and nitrogen derivatives that can be taken up easily by the surviving population. PCD is believed to be a survival mechanism, for which some cells respond to a nutrient starvation period by committing suicide and releasing essentials nutrients into the medium. Thus, during PCD, cells can degrade nucleotides into urea and ammonium in response to, for example, nitrogen limitation. This may explain the lack of negative regulation in the allantoin pathway by nitrogen metabolites. Together, these results expand our understanding of primary and secondary metabolism in *Streptomyces* and bridge a gap between secondary and primary metabolism in this fascinating bacterial family.

Acknowledgments This work was supported by ANPCyT grants PICT 2007–00711 to PC and PICT2008-644 to HG, Fundación Perez-Guerrero grant to ER and PIP 100764 from CONICET to ER. ER, PC, and HG are members of the Research Career and LN is a doctoral fellow of CONICET. CLC is a doctoral fellow of CONACYT. We kindly thank Dr. Alun Jones and Dr. Amanda Nouwens for LC-MS assistance and David Hopwood for helpful comments. All proteomics work was performed at the proteomics facility at IMB and/or SCMB. We thank Paul Dyson (Swansea University) for kindly providing the derivative cosmids carrying transposon insertions and Monica Hourcade (Universidad Nacional de Rosario) for technical assistance in the metabolomic analysis.

Conflict of interest The authors declare no competing financial interests.

References

Ashiuchi M, Misono H (1999) Biochemical evidence that *Escherichia coli hyi* (orf b0508, gip) gene encodes hydroxypyruvate isomerase. Biochim Biophys Acta 1435(1–2):153–159

Bentley SD, Chater KF, Cerdeno-Tarraga AM, Challis GL, Thomson NR, James KD, Harris DE, Quail MA, Kieser H, Harper D, Bateman A, Brown S, Chandra G, Chen CW, Collins M, Cronin A, Fraser A, Goble A, Hidalgo J, Hornsby T, Howarth S, Huang CH, Kieser T, Larke L, Murphy L, Oliver K, O'Neil S, Rabbinowitsch E, Rajandream MA, Rutherford K, Rutter S, Seeger K, Saunders D, Sharp S, Squares R, Squares S, Taylor K, Warren T, Wietzorrek A, Woodward J, Barrell BG, Parkhill J, Hopwood DA (2002) Complete genome sequence of the model actinomycete *Streptomyces coelicolor* A3(2). Nature 417(6885):141–147

Brana AF, Wolfe S, Demain AL (1985) Ammonium repression of cephalosporin production by *Streptomyces clavuligerus*. Can J Microbiol 31(8):736–743

Brana AF, Wolfe S, Demain AL (1986) Relationship between nitrogen assimilation and cephalosporin synthesis in *Streptomyces clavuligerus*. Arch Microbiol 146(1):46–51

Bystrykh LV, Fernandez-Moreno MA, Herrema JK, Malpartida F, Hopwood DA, Dijkhuizen L (1996) Production of actinorhodin-related "blue pigments" by *Streptomyces coelicolor* A3(2). J Bacteriol 178(8):2238–2244

Doull JL, Vining LC (1990) Nutritional control of actinorhodin production by *Streptomyces coelicolor* A3(2): suppressive effects of nitrogen and phosphate. Appl Microbiol Biotechnol 32(4):449–454

Gupta NK, Vennesland B (1964) Glyoxylate carboligase of *Escherichia coli*: a flavoprotein. J Biol Chem 239:3787–3789

Herron PR, Hughes G, Chandra G, Fielding S, Dyson PJ (2004) Transposon Express, a software application to report the identity of insertions obtained by comprehensive transposon mutagenesis of sequenced genomes: analysis of the preference for in vitro Tn5 transposition into GC-rich DNA. Nucleic Acids Res 32(14):e113

Hobbs G, Frazer CM, Gardner DCJ, Flett F, Oliver SG (1990) Pigmented antibiotic production by *Streptomyces coelicolor* A3(2): kinetics and the influence of nutrients. Microbiology 136:2291–2296

Hodgson DA (2000) Primary metabolism and its control in streptomycetes: a most unusual group of bacteria. Adv Microb Physiol 42:47–238

Kieser T, Bibb MJ, Buttner MJ, Chater KF, Hopwood DA (2000) Practical *Streptomyces* genetics, 2000th edn. Norwich, UK

Loewen PC, Switala J (1986) Purification and characterization of catalase HPII from *Escherichia coli* K12. Biochem Cell Biol 64(7):638–646

Loke P, Sim TS (2000) Molecular cloning, heterologous expression, and functional characterisation of a malate synthase gene from *Streptomyces coelicolor* A3(2). Can J Microbiol 46(8):764–769

Manteca A, Mader U, Connolly BA, Sanchez J (2006) A proteomic analysis of *Streptomyces coelicolor* programmed cell death. Proteomics 6(22):6008–6022

McInnch JK, McInnch JD, May SW (2003) Catalysis, stereochemistry, and inhibition of ureidoglycolate lyase. J Biol Chem 278(50): 50091–50100

Molina I, Pellicer MT, Badia J, Aguilar J, Baldoma L (1994) Molecular characterization of *Escherichia coli* malate synthase G. Differentiation with the malate synthase A isoenzyme. FEBS J 224(2):541–548

Mulrooney SB, Hausinger RP (2003) Metal ion dependence of recombinant *Escherichia coli* allantoinase. J Bacteriol 185(1):126–134

Njau RK, Herndon CA, Hawes JW (2000) Novel beta -hydroxyacid dehydrogenases in *Escherichia coli* and *Haemophilus influenzae*. J Biol Chem 275(49):38780–38786

Nygaard P (1983) Utilization of preformed purine bases and nucleosides. In: Munch-Petersen A (ed) Metabolism of nucleotides, nucleosides and nucleobases in microorganisms. Academic, London, UK, pp 27–93

Ohe T, Watanabe Y (1979) Purification and properties of xanthine dehydrogenase from *Streptomyces cyanogenus*. J Biochem 86(1):45–53

Ohe T, Watanabe Y (1980) Purification and properties of hypoxanthine phosphoribosyltransferase from *Streptomyces cyanogenus*. Agric Biol Chem 44(9):1999–2006

Ohe T, Watanabe Y (1981) Purification and properties of urate oxidase from *Streptomyces cyanogenus*. J Biochem 89(6):1769–1776

Omura S, Oiwa R (1984) Studies on bioactive compounds from microorganisms. Kitasato Arch Exp Med 57(2):75–204

Omura S, Tanaka Y, Mamada H, Masuma R (1983) Ammonium ion suppresses the biosynthesis of tylosin aglycone by interference with valine catabolism in *Streptomyces fradiae*. J Antibiot (Tokyo) 36(12):1792–1794

Pfaffl MW (2001) A new mathematical model for relative quantification in real-time RT-PCR. Nucleic Acids Res 29(9):e45

Piedras P, Munoz A, Aguilar M, Pineda M (2000) Allantoate amidinohydrolase (Allantoicase) from *Chlamydomonas reinhardtii*: its purification and catalytic and molecular characterization. Arch Biochem Biophys 378(2):340–348

Ramazzina I, Cendron L, Folli C, Berni R, Monteverdi D, Zanotti G, Percudani R (2008) Logical identification of an allantoinase analog (*puuE*) recruited from polysaccharide deacetylases. J Biol Chem 283(34):23295–23304

Rodriguez E, Hu Z, Ou S, Volchegursky Y, Hutchinson CR, McDaniel R (2003) Rapid engineering of polyketide overproduction by gene transfer to industrially optimized strains. J Ind Microbiol Biotechnol 30(8):480–488

Rodriguez E, Navone L, Casati P, Gramajo H (2012) Impact of malic enzymes on antibiotic and triacylglycerol production in *Streptomyces coelicolor*. Appl Environ Microbiol 78(13):4571–4579

Schultz AC, Nygaard P, Saxild HH (2001) Functional analysis of 14 genes that constitute the purine catabolic pathway in *Bacillus subtilis* and evidence for a novel regulon controlled by the PucR transcription activator. J Bacteriol 183(11):3293–3302

Shen YQ, Heim J, Solomon NA, Wolfe S, Demain AL (1984) Repression of beta-lactam production in *Cephalosporium acremonium* by nitrogen sources. J Antibiot (Tokyo) 37(5):503–511

Shilov IV, Seymour SL, Patel AA, Loboda A, Tang WH, Keating SP, Hunter CL, Nuwaysir LM, Schaeffer DA (2007) The Paragon Algorithm, a next generation search engine that uses sequence temperature values and feature probabilities to identify peptides from tandem mass spectra. Mol Cell Proteomics 6(9):1638–1655

Takada Y, Noguchi T (1983) The degradation of urate in liver peroxisomes. Association of allantoinase with allantoicase in amphibian liver but not in fish and invertebrate liver. J Biol Chem 258(8):4762–4764

Trijbels F, Vogels GD (1966) Allantoicase and ureidoglycolase in *Pseudomonas* and *Penicillium* species. Biochim Biophys Acta 118(2):387–395

Tsao SW, Rudd BA, He XG, Chang CJ, Floss HG (1985) Identification of a red pigment from *Streptomyces coelicolor* A3(2) as a mixture of prodigiosin derivatives. J Antibiot (Tokyo) 38(1):128–131

Vogels GD, Van der Drift C (1976) Degradation of purines and pyrimidines by microorganisms. Bacteriol Rev 40(2):403–468

Wang P, Kong CH, Hu F, Xu XH (2007) Allantoin involved in species interactions with rice and other organisms in paddy soil. Plant Soil 296(1–2):43–51

Wang P, Kong C, Sun B, Xu X (2010) Allantoin-induced changes of microbial diversity and community in rice soil. Plant Soil 332(1–2):357–368

Watanabe Y (1971) Studies on the formation of uricase by *Streptomyces*. Part III. The Effect of incubation with or without purines. Agric Biol Chem 35(13):2008–2014